Sensors & Actuators: A. Physical 376 (2024) 115586

Contents lists available at ScienceDirect

Sensors and Actuators: A. Physical

journal homepage: www.journals.elsevier.com/sensors-and-actuators-a-physical

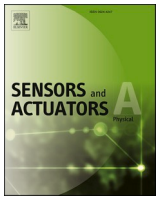

Pedestrian detection using a MEMS acoustic array mounted on a moving vehicle

Alberto Izquierdo, Lara del Val *, Juan José Villacorta

Signal Theory and Communications and Telematics Engineering Department, University of Valladolid, Valladolid 47011, Spain

ARTICLE INFO

Keywords:
Pedestrian detection
MEMS microphone array
Onboard system
Moving vehicle

ABSTRACT

Automatic pedestrian detection in a vehicle is of vital importance in Advanced Driver Assistance Systems (ADAS). Sensors currently used are based on cameras, radars and lidars, whose performance is degraded in environments with reduced visibility: night, smoke, fog, etc. This paper has validated the use of an active array of 150 MEMS (Micro-Electro Mechanical Systems) microphones incorporated into a conventional car moving in real urban traffic conditions, with the system working in real time, at a rate of 8 detections per second. Together with beamforming, Constant False Alarm Rate (CFAR) detection and lane detection algorithms, a crucial algorithm has been incorporated for the proper performance of the system that discriminates the detections of objects or pedestrians generated by the system from the false alarms generated by road imperfections, such as bumps, cracks, etc. Based on 6000 captures, performed with the car moving at 30 km/h, which is the typical speed limit in urban environments, it has been possible to detect pedestrians positioned at a distance from the car varying between 5 and 20 m, with a detection probability of 0.91 and a false alarm probability of 0.01. The results obtained have validated the effectiveness of using active acoustic arrays in the field of pedestrian detection and position estimation from moving cars in urban environments. The fusion of the presented system with the systems currently used for this purpose, would significantly improve the performance of pedestrian detection systems interacting with AEB (Automatic Emergency Breaking) systems, extending their operability to environments with reduced visibility, and resulting in the reduction in the number of possible collisions with pedestrians, thus increasing their safety.

1. Introduction

Due to the widespread use of road vehicles, the number of traffic accidents and collisions per year is at around 1.35 million. In fact, 23 % of these accidents are associated with pedestrian fatalities, leading to more than 300,000 pedestrian deaths each year [1]. Nowadays, the automotive and transport sectors work actively to reduce this fatal number, which is more evident in urban environments, where the presence of pedestrians is higher. The search for solutions to this problem has been boosted by the development of the autonomous car, where it is use in these urban environments for the same reason.

Over the last decades, in the search of these solutions, many vehicles (autonomous or not) have been equipped with Advanced Driver Assistance Systems (ADAS), in order to improve the comfort, efficiency, and safety of the vehicles. One of these systems, the AEB-P (Autonomous Emergency Braking for Pedestrians), is specifically focused on pedestrian detection [2–7].

In the different actions that are being performed to reduce the number of accidents involving pedestrians, it is essential to carry out studies and developments to improve pedestrian detection algorithms and/or systems. Studies based on improving detection algorithms are focused on using statistical models [8], improving algorithms for tracking detected pedestrians [9–12], on defining complex scenarios [13], using contour features [14–17], or on using machine learning algorithms [18,19]. Currently, most of the systems used for pedestrian detection are based on RGB (Red-Green-Blue) cameras and image processing algorithms. The problem with these systems is that they only are effective with adequate visibility conditions, so that there are many studies which are trying to solve this problem. Some of these potential solutions are based on developing pedestrian detection algorithms in low visibility environments (fog, rain, night) [20–22], and others focus on using different detection systems, such as infrared sensors [23–25], LIDARs (Laser Imaging Detection and Ranging) [26–30], ultrasonic sensors [31,32], RFID (Radio Frequency IDentification) [33,34], or

* Corresponding author.
E-mail address: lara.val@uva.es (L. del Val).

https://doi.org/10.1016/j.sna.2024.115586
Received 7 November 2023; Received in revised form 22 May 2024; Accepted 7 June 2024
Available online 14 June 2024

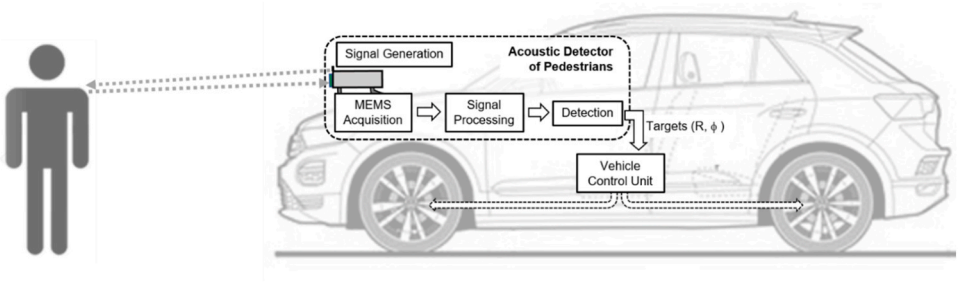

Fig. 1. System block diagram.

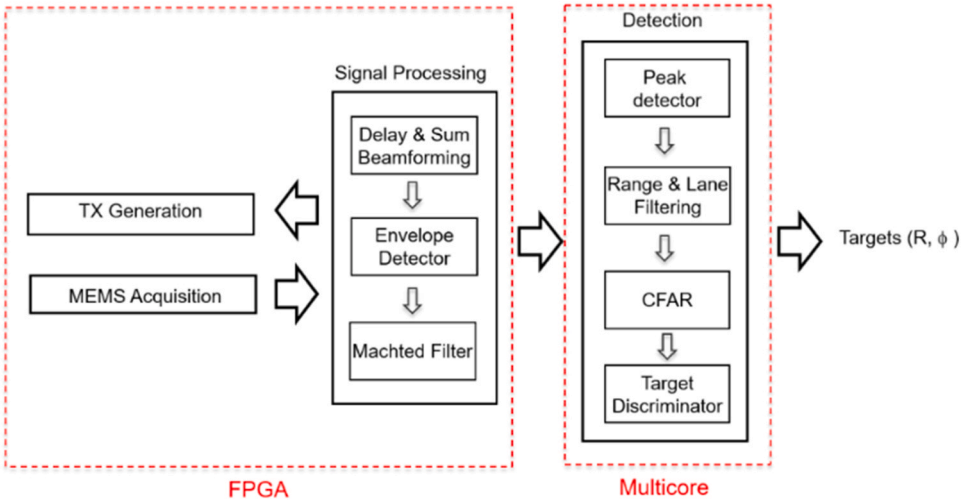

Fig. 2. Processing algorithms.

RADARs (Radio Detection And Ranging) [35,36]; or systems fusing a classic RGB camera with another detection system (thermal camera [22, 37,38], LIDAR [39,40], or microphone array [41]).

Particularly, the work shown in this paper is based on the idea of using an acoustic array mounted on a moving vehicle in order to detect pedestrians to prevent traffic accidents. The advantage of using an acoustic system is that its performance is not impaired if the surrounding visibility is reduced. The acoustic array used in this work is composed of MEMS (Micro-Electro-Mechanical Systems) microphones, and on the authors' experience in the development of acoustic arrays for human detection [42–45].

In one of these previous works [45], the authors studied and demonstrated the feasibility of using an acoustic system, based on an acoustic array of microphones, to detect and estimate the position of a person. In that work, the performance of the acoustic array was evaluated, as well as the algorithms for the acquisition, beamforming and detection, based on a CFAR (Constant False Alarm Rate) scheme and a lane filter, tasks. In that study, the system, located on a fixed position, not mounted on a car, was used to generate and transmit the acoustic signals and, after their reflection over the person, to acquire the reflected signals and to send them to a personal computer (PC), where the acquired signals were stored for subsequent off-line processing. Except for the MEMS sensors acquisition tasks, which were implemented in the FPGA (Field Programmable Gate Array), the processing algorithms associated to the detection system were implemented off-line on the external PC.

This contribution deals with the analysis of the system under real conditions of use, which implies: i) Implementing the system in real time, allowing its integration with the vehicle's AEB system, so that it can detect the pedestrian quickly enough, depending on the speed at which the car is moving, so that the car can stop in time to avoid hitting the pedestrian; ii) Embedding and mounting the system on a real car, optimizing the position of the acoustic array outside the vehicle; iii) Analyzing the performance of the system mounted on a moving vehicle, taking into account the corresponding problems related with real noises: engine, rolling, wind, road imperfections, etc. As it was mentioned previously, the final objective of pedestrian detection is to pass the pedestrian's position information to the vehicle's control unit, to alert the AEB system, so that it can decide whether or not to brake the car. This acoustic pedestrian detection system could serve as a support system for those detection systems that are already incorporated as ADAS systems in vehicles, in order to improve their performance in environments with reduced visibility. This improved performance would increase pedestrian safety, reducing the number of possible collisions.

Section 2 presents a description of the system employed in this study, showing the solutions implemented on the system in order to assure that the system work properly under real-time working conditions and being embedded on a moving vehicle. Section 3 presents the results obtained on the tests and their corresponding discussion. Finally, Section 4 shows the conclusions drawn by the authors with the obtained results.

2. System description

2.1. System functional description

The acoustic system developed for pedestrian detection has the next characteristics, that can be observed in Fig. 1:

- It is mounted on the front part of the vehicle, because its main objective is the detection of pedestrians in the vehicle's path.
- As this is an active system, based on the RADAR principle, it needs to transmit, or to generate, an acoustic signal, that will be reflected on

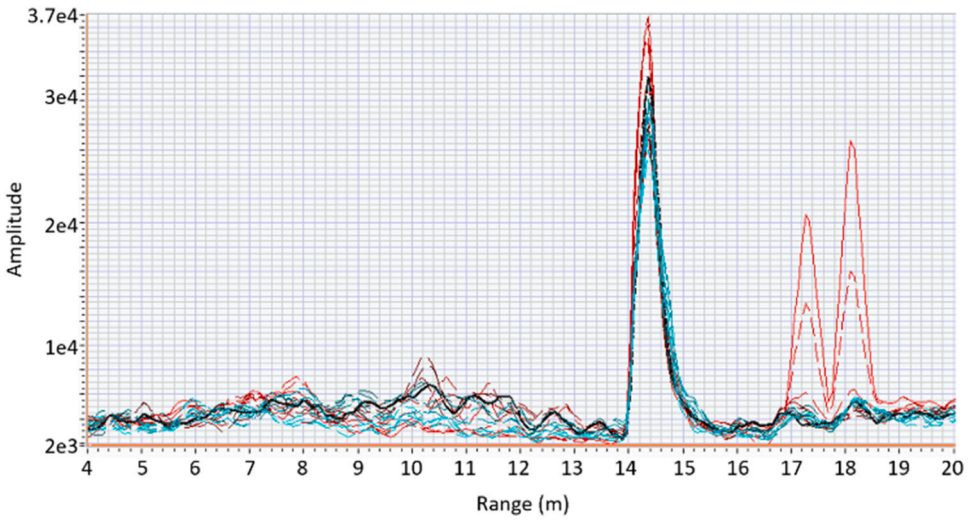

Fig. 3. False detections in captured signals.

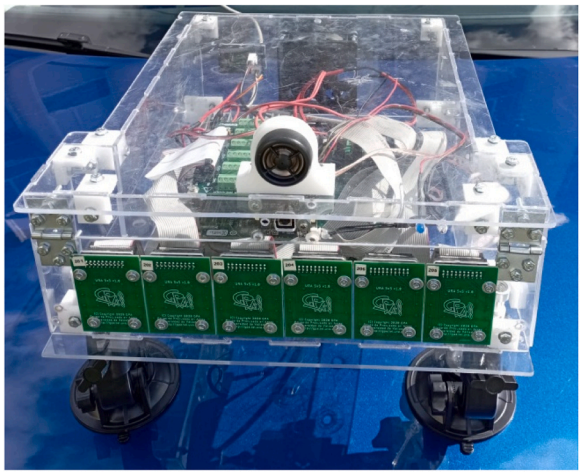

Fig. 4. Acquisition system.

the pedestrian. In this case, a tweeter has been employed as the transmission system.

- The reflected signal will be acquired by an array of digital MEMS microphones (to receive the signal reflected on the pedestrian). Specifically, the acoustic acquisition block of the system is based on a rectangular array of 5×30 MEMS microphones uniformly spaced every 0.9 cm.
- The 150 acoustic signals captured by the microphones of the array will be processed on the basis of a Delay & Sum beamforming algorithm to generate a discrete set of beams to cover the vehicles' path, as it will be the corresponding surveillance space.
- The relative maxima of each beam will be identified, taking into account, as potential targets, only the ones included inside the detection lane. And after that, these detections will be validated.
- In case of detection, the system will communicate with the vehicle's control unit to alert the AEB system or the corresponding ADAS system. Given that AEB systems usually work in urban environments, the pedestrian detection should work properly with the vehicle moving within urban speed limits.
- The base unit of the processing and detection subsystems employed in this work is a National Instruments sbRIO (Single Board Reconfigurable Input/Output) 9629 board, based on a FPGA Artix-7 200 T and a Quad-Core Intel Atom processor.

2.2. *Real-time implementation of the algorithms*

Based on the algorithms used in previous works by the authors described in [45], a complete reimplementation has been carried out

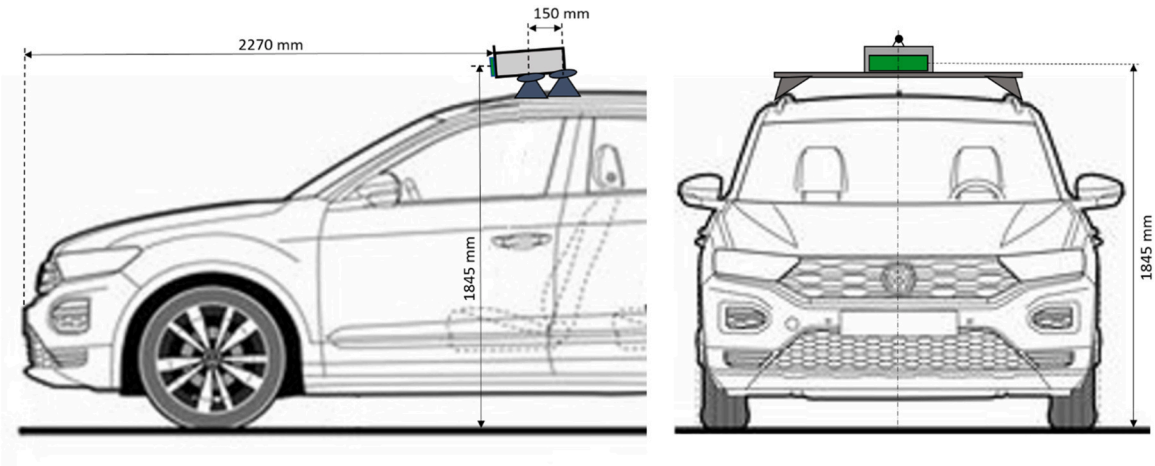

Fig. 5. First assembly diagram.

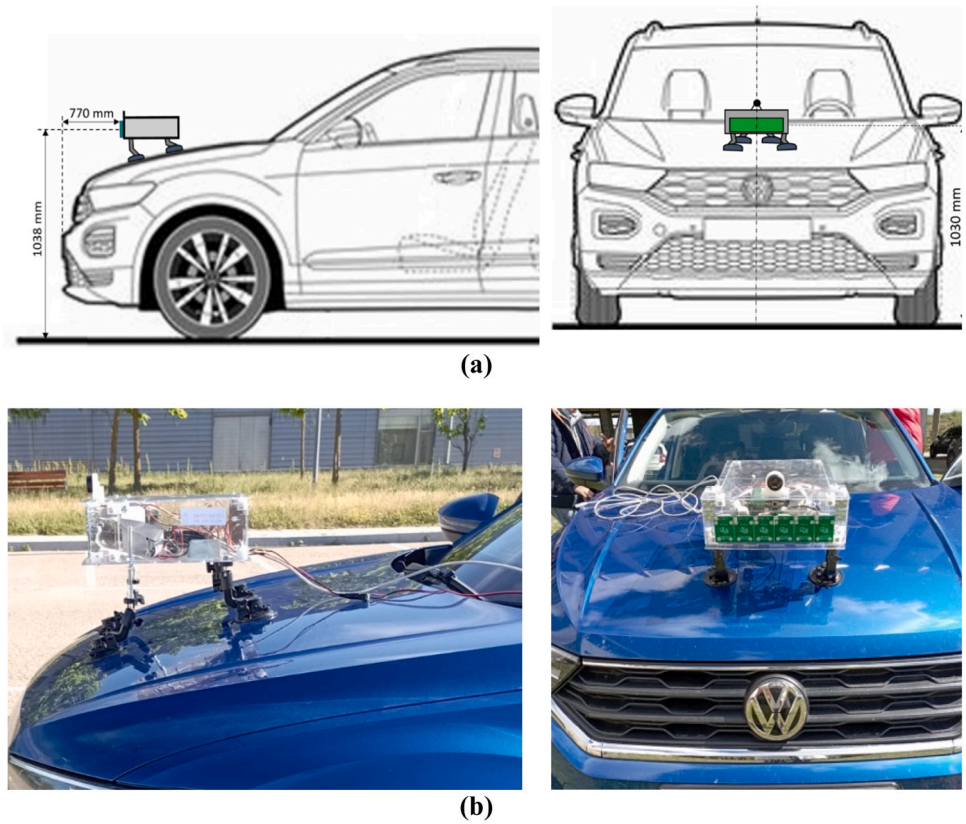

Fig. 6. On-vehicle system final installation: (a) diagrams and (b) photographs.

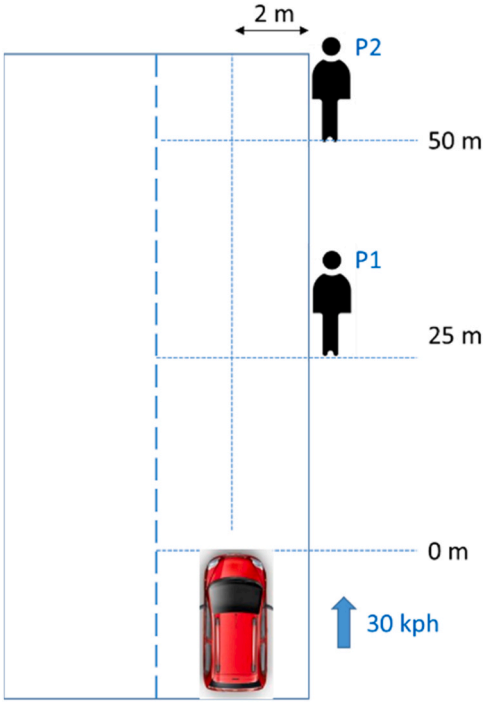

Fig. 7. Diagram of the roadway for the tests.

with the aim of achieving real-time operation, for which the algorithms have been distributed among the processing units included in the sbRIO 9629 card, the FPGA and the Atom cores, or multicore, as shown in Fig. 2. The modular design of the previously defined algorithms has allowed the current implementation to focus on the problems associated with parallelization and real-time execution, without increasing the computational complexity of the system significantly.

In the Field Programmable Gate Array (FPGA), which allows the implementation of multiple processing paths in parallel, the first processing stages have been implemented. The specific blocks implemented in the FPGA are:

- **Transmission block**
  It is in charge of synthesizing a pulsed signal that will be transmitted by the tweeter, after passing through a power amplifier. The transmitter generates two analog pulses separated in time by a preset value known by the detector. The purpose of generating this particular pulsed signal is to subsequently discriminate in the detector whether the reflected signals come from the transmitter or are the result of an external source.
  The transmitted signal is repeated every 125 ms, that is at a rate of 8 transmissions per second (8 FPS or Frames per Second), which allows the detection of targets at a maximum distance of 21 m, taking into account the sound propagation speed.
- **Acquisition block**
  It is in charge of the synchronous acquisition of the 150 signals received by the MEMS microphones.
- **Signal processing block**

It is in charge of mixing the signals captured by each microphone and generating a signal containing the information coming from each pointing direction called beam. It is composed of three subsystems: a beamformer, an envelope detector and a matched filter.

- The beamformer based on the Delay & Sum algorithm processes the 150 signals captured in the microphone array and generates a set of 17 discrete beams equispaced in azimuth 3º covering from −24º to

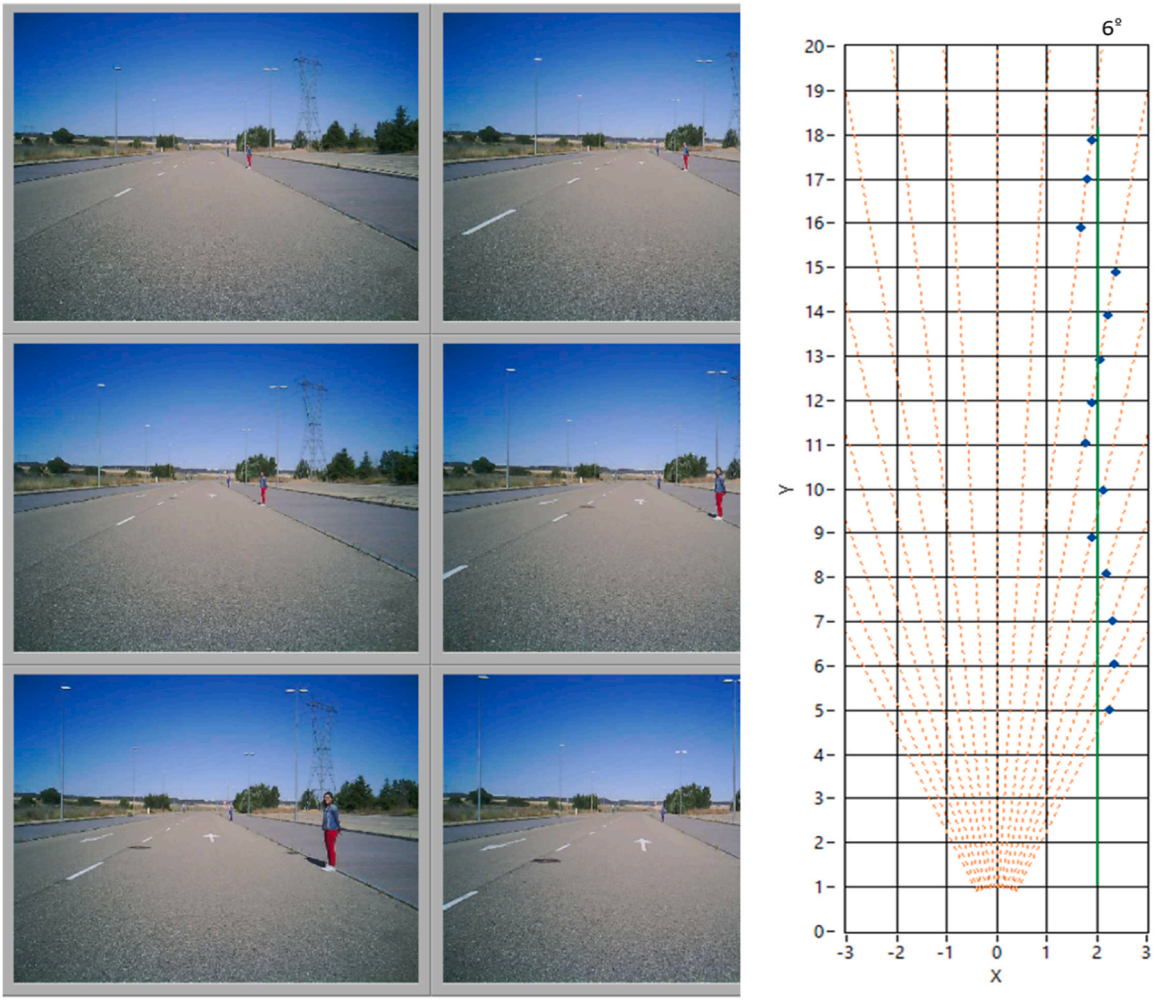

Fig. 8. Detections for a specific trip.

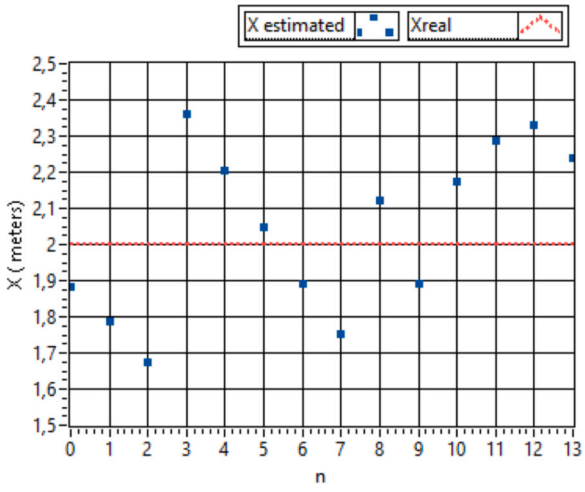

Fig. 9. Estimated vs. real X-coordinate values of the pedestrian position.

24º with a fixed elevation angle of 0º, since the pedestrian is on the same surface on which the car is moving and the array is designed to have a large beamwidth in elevation.

- The envelope detector of the beamformed signals allows the system to be invariant to the Doppler effect.

Table I
Detection and False Alarm Probabilities for Pedestrians at Different Ranges.

Pedestrian range (m)	Captures	Detections	True detections	False alarms	Pd	Pfa
5–7.5	873	713	701	12	0.80	0.014
7.5–10	891	793	779	14	0.87	0.016
10–12.5	896	807	802	5	0.90	0.006
12.5–15	865	807	800	7	0.92	0.008
15–17.5	917	893	887	6	0.97	0.007
17.5–20	862	848	839	9	0.97	0.010
20–21	386	364	357	7	0.92	0.018
Total	5690	5225	5165	60	0.91	0.011

- The matched filter processes the envelope of each beampattern by means of a matched filter whose impulse response is the envelope of the transmitted pulse and which maximizes the SNR (Signal-to-Noise Ratio) prior to detection.

The processing of each of the 17 beams is carried out simultaneously and with minimal delay thanks to the parallelism capability of the FPGA.

These beams are transferred to the main memory for further processing in the Atom cores included in the sbRIO board where the last block, the detection block, is implemented.

- **Detection block**

This block is responsible for identifying target detections from the beams and it is composed of four subsystems: a peak detector, a distance and lane filter, a CFAR (Constant False Alarm Ratio) detector and a target discriminator.

- The peak detector identifies, for each of the beams, the range of the relative maxima that have exceeded a minimum detection threshold. It generates a list of detected targets identified by their range and azimuth.
- The range and lane filter eliminates all those targets that are neither within the detection range of the vehicle nor within the lane in which the vehicle is moving. The detection range is defined between 5 m and 21 m and the lane width as typically 4 m.
- The CFAR detector analyzes in a range and azimuth environment, for each target, the value of the energy adjacent to the detected maxima, generating an adaptive threshold that is compared with the value of the detected target. If the value of the detected target is higher than the adaptive threshold value, the detection is validated, and if it is lower, the detection is eliminated.
- A target discriminator validates whether each of the detections corresponds to a pulse emitted by the system or an external noise source. Since the transmitter has sent two identical pulses with a pre-established separation, the discriminator evaluates whether there are two consecutive detections with the defined separation. If there are, the two detections are merged into a single detection and if there aren't, the detection is discarded as it is produced by an external signal that was not sent by the transmitter.

This last algorithm was not present in previous works and has been introduced, after the first tests carried out, to reduce the number of false alarms due to wheel noise when crossing road cracks as explained in the following Section 2.3.

The real-time operating system of the sbRIO board allows each of the above algorithms to run at a specific core so that the delay is reduced and the jitter is controlled.

2.3. Road imperfections/target discrimination algorithm

In the first dynamic tests carried out, the developed system was mounted on the vehicle and was driven along different roads at a, more or less, constant speed, in order to qualitatively verify the system's performance. In these first experiments, it was found that the system was able to detect objects and people located on the edges of the road as the vehicle approached them. However, it was also observed that the number of false detections was considerably higher than those obtained in previous static tests. In the static tests, false alarm probability (Pfa) values between 0.006 and 0.018 were obtain [45], whereas in these first new tests Pfa values around 0.45 where obtained.

Subsequent analysis of the signals captured with the vehicle in motion showed that these false detections were shown as large amplitude pulses, such as the ones shown in Fig. 3 between 14 and 15 m, affecting all the 17 beams defined on the Delay & Sum beamforming processing step. In this Fig. 3, each colored curve represents one of these beams.

After several additional tests and analyses, it was concluded that these pulses were due to the noise produced by the wheels passing over the asphalt cracks crossing the road. The problem in this case was that the width of these pulses was similar to the echo of the pulse emitted by the system and reflected by an object, so the CFAR-based detector could not distinguish them from a real echo, arising false detections.

Analyzing the road section selected for testing the system, it was detected that there were 10 cracks distributed along it. After about 20 passes of the car along the road, a total of 467 detections were obtained, so that 447 of them were false, defining the Pfa value of 0.447 previously indicated.

In order to discriminate these false detections from the desired ones, the authors chose to send, as the acoustic transmission signal of the active system, a signal composed of two pulses so that each real target produced two consecutive detections in the same beam while the noise due to the crosses over the asphalt cracks produced only one detection. This effect is shown in Fig. 3, where these two consecutive detections are shown between 17 and 19 m, and the detection due to a crack is shown between 14 and 15 m, as it was mentioned previously.

As explained in Section 2.2, the corresponding road imperfection/target discriminator block has been implemented after the CFAR detector to identify and eliminate these false detections due to imperfections that can be present on the road. Each detection is analyzed, looking for another subsequent detection in the same beam that should be separated a gap time the two emitted pulses. If not found, the detection is assumed to be caused by a crack on the road and is discarded.

3. Results

3.1. On-vehicle system installation

As previously mentioned, one of the most important characteristics of the developed system is that it had to be onboard a vehicle. In order to carry out the system tests, a compact system has been developed, with all its components included in a box, as shown in Fig. 4.

This box has the corresponding transmission (tweeter) and acquisition (MEMS array) systems installed on the outside, as well as a network cable to connect the system via Ethernet with a control system implemented, in this test version, in a laptop, and a power cable, connected in the tests to an external battery.

As a first approximation to the test, it was decided to place the system on the roof of the car, emulating the LIDAR positioning in the current autonomous cars being developed by companies such as Google, Xiaomi or Tesla. A schematic diagram of this first setup defined for the system is shown in Fig. 5. In this first setup, to attach the system to the roof of the vehicle, a pair of luggage carrier crossbars were used.

After carrying out the first tests, it was found that this assembly caused problems because the transmitted acoustic signal bounced off the junction of the hood of the car with the front window, causing the presence of interfering signals in the system. The cause of this effect is that the signal beamwidth in elevation is too wide due to the small spatial aperture of the array in that dimension. To solve this problem, it was finally decided to place the system at the front of the vehicle, as it is shown in the diagrams and photographs in Fig. 6. For this particular assembly, suction cups and screws were used to fix the system parallel to the road on the hood of the car.

It is worth noting that this placement of the system is for the test prototype. In a possible final system, the array and processing system would be integrated into the car. For example, with the array integrated in the front ventilation grille, and the processing system inside the vehicle, together with the rest of the processing elements available.

3.2. Tests description

For the qualitative evaluation of the system, the tests have been carried out in a real scenario based on a 2-lane avenue with a total width of 8 m, and a length of several hundred meters so that the car can travel at a constant speed. In this scenario, 2 people have been placed 25 m apart and positioned on the right edge of the lane. Two people have been used to increase the number of detections on each pass. Since AEB systems are often used in urban environments, and many cities are reducing speed limit in urban environments to 30 km/h, in these tests, the vehicle passes through the center of its lane with a constant speed of 30 km/h (managed by the car's speed control system). For safety reasons the pedestrian remains stationary in position. A diagram of the roadway can be found in Fig. 7.

The vehicle has made a total of 200 trips, performed in 5 sessions, with a cadence of 8 acoustic images, or frames, per second, on which a statistical analysis has been performed to evaluate the detection and

false alarm probabilities as functions of the pedestrian's range. The position of the vehicle for each of the acoustic captures was obtained using a differential GPS (Global Positioning System) with RTK (Real Time Kinematic), and since the fixed position of each pedestrian is known, the range between the car and the pedestrian was calculated.

Considering that the system detects the pedestrian in the range of 5–21 m and that the vehicle speed is 30 km/h, equivalent to 8.4 m/s, a time window of 1.9 s is available, where between 14 and 15 detections should be obtained for each pedestrian in each pass.

3.3. Tests results

Fig. 8 shows the detections for a specific trip in front of pedestrian P1, while 6 images equispaced in range have been selected. The detections are displayed as blue dots in Cartesian coordinates, while the steering angles of the beams where they have been detected are represented by red dashed lines.

It can be observed that as the pedestrian is closer to the vehicle, the steering angle increases from 6º to 24º. Logically, since the beams are defined in 3º intervals, there is an error in the estimation of the X coordinate. Fig. 9 shows the estimated values of the X coordinate in relation to the real position of the pedestrian (2 m). These errors have been taken into account when defining the lane filter parameters.

3.4. Analysis of the detection and false alarm probabilities

Based on the set of experiments developed and given that for each experiment the position of the vehicle in relation to the pedestrian is known, the detection probability (Pd) and the false alarm probability (Pfa) have been estimated. For this purpose, the detections made for each of the pedestrians in a range between 5 and 21 m have been processed, defining 7 intervals of 2.5 m, although the last interval would only be 1 m wide.

In theory, as the vehicle has made a total of 200 trips moving at 8.4 m/s, the system should have performed between 5600 and 6000 captures, related with the theoretical 14–15 detections defined for each vehicle pass. In practice, 5690 captures were obtained in which 5225 detections were made, of which 5165 were correct and 60 were false alarms. Therefore, the average acoustic detection system has a Pd=0.91 and a Pfa=0.011.

Comparing the results obtained in the publication "Feasibility of Using a MEMS Microphone Array for Pedestrian Detection in an Autonomous Emergency Braking System" [32], where the system was analyzed with the vehicle stopped and a pedestrian at different distances, with a Pd=0.99 and a Pfa=0.01, it is observed that in this new dynamic scenario the Pfa is equivalent, while Pd decreases notably.

We have to consider that the acoustic radar is traveling at a speed of 30 km/h and therefore additional noise contributions are generated, among them: the noise generated by the vehicle engine, the rolling noise and the noise produced by the wind flow. The detector based on a CFAR algorithm adequately controls the value of the false alarm probability at the cost that the detection probability decreases, since in this dynamic scenario the SNR is significantly lower.

Performing a more detailed analysis for each of the range intervals yields the results in Table I.

It is observed that the probability of detection decreases for close ranges where the clutter associated with the road is very significant as well as for far ranges where the reflected pulse energy is lower. In relation to the false alarm probability, it increases for close ranges due to the presence of the clutter as well as for far ranges, where the signal to noise ratio (SNR) is lower.

4. Conclusions

A pedestrian detection system based on an active acoustic array has been evaluated under real operating conditions, i.e.: i) mounted on a vehicle moving in an urban environment, ii) real-time processing of all the acquisition, beamforming and localization algorithms, and iii) taking into account real conditions: rolling noise, engine sound, clutter and road imperfections, etc.

In this work, a detailed description of the algorithms implemented in real time, both in the FPGA and in the Atom processors of the used sbRIO board, is presented. An algorithm has been specifically designed to drastically reduce the false alarms produced by cracks and discontinuities in the road. Also, two positions for the acoustic radar in the car have been evaluated to reduce the effects of clutter caused by the road surface.

Finally, for a dynamic scenario with speeds of 30 km/h and performing 5690 captures, the detection (Pd) and false alarm (Pfa) probabilities of the system have been evaluated, obtaining average values of Pd=0.91 and Pfa =0.011. The degradation of the system performance at short distances, due to the clutter of the road, and at long distances, due to the loss of SNR, have been studied. These results revalidate the feasibility of the system under real conditions has been revalidated.

Additionally, a set of actions, as future work, are proposed to improve the system performance: (i) Increasing the power/bandwidth of the emitted signals that enable an increase in SNR and therefore an increase in the detection probability; (ii) applying statistically optimal beamforming algorithms that cancel to a greater degree the clutter associated with the road and (iii) applying tracking and track association techniques based on Kalman filters that allow correlating the information of multiple detections associated with the same target, increasing the cumulative detection probability while decreasing the false alarm probability.

CRediT authorship contribution statement

Lara del Val: Methodology, Validation, Visualization, Writing – original draft, Writing – review & editing. **Juan José Villacorta:** Investigation, Software, Validation, Visualization. **Alberto Izquierdo:** Conceptualization, Formal analysis, Methodology, Validation, Visualization.

Declaration of Competing Interest

The authors declare the following financial interests/personal relationships which may be considered as potential competing interests: Alberto Izquierdo, Lara del Val and Juan J. Villacorta reports financial support was provided by Spanish Science, Innovation and Universities Ministry. If there are other authors, they declare that they have no known competing financial interests or personal relationships that could have appeared to influence the work reported in this paper

Data Availability

Data will be made available on request.

Acknowledgements

This work was supported by the Spanish Science, Innovation and Universities Ministry, under Grant RTI2018–095143-B-C22.

References

[1] World Health Organization, Technical Documents. WHO: Geneva, Switzerland. *Global Status Report on Road Safety 2018: Summary*, ⟨https://apps.who.int/iris/handle/10665/277370⟩; 2018 [accessed 10 January 2023].

[2] Liu Z., Ma W., Liu W., Zhang S. Research on Calibration Technology of AEB Target Pedestrian Dummy Based on Radar and Infrared Reflected Signal. In: Proc 13th International Conference on Measuring Technology and Mechatronics Automation, Beihai, China; 16-17 Jan. 2021, p. 295-300.

[3] B.J. Kim, S.B. Lee, A study on the evaluation method of autonomous emergency vehicle braking for pedestrians test using monocular cameras, Appl. Sci. 10 (13) (2020) 4683, https://doi.org/10.3390/app10134683.

[4] A. López-Rosado, S. Chien, L. Li, Q. Yi, Y. Chen, R. Sherony, Certainty and critical speed for decision making in tests of pedestrian automatic emergency braking systems, IEEE Trans. Intell. Transp. Syst. 18 (6) (2017) 1358–1370, https://doi.org/10.1109/TITS.2016.2603445.
[5] M. Park, S. Lee, C. Kwon, S. Kim, Design of pedestrian target selection with funnel map for pedestrian AEB system, IEEE Trans. Veh. Technol. 66 (5) (2017) 3597–3609, https://doi.org/10.1109/TVT.2016.2604420.
[6] Z. Abdullah, P.M. Heerwan, M.A. Zakaria, M.I. Ishak, investigation of the combination of kinematic path planning and artificial potential field path planning with PI controller for autonomous emergency braking pedestrian (AEB-P) system. Enabling Industry 4.0 through Advances in Mechatronics Lecture Notes in Electrical Engineering, Springer, Singapore, 2022.
[7] H.K. Lee, S.G. Shin, D.S. Kwon, Design of emergency braking algorithm for pedestrian protection based on multi-sensor fusion, Int. J. Automot. Technol. 18 (2017) 1067–1076, https://doi.org/10.1007/s12239-017-0104-7.
[8] S. Zhang, C. Bauckhage, A.B. Cremers, Efficient pedestrian detection via rectangular features based on a statistical shape model, IEEE Trans. Intell. Transp. Syst. 16 (2) (2015) 763–775, https://doi.org/10.1109/TITS.2014.2341042.
[9] J.H. Choi, K.J. Lee, S. Oh, K. Nam, Development of vehicle maneuvering system for autonomous driving, Mechatronics 85 (2022) 102798, https://doi.org/10.1016/j.mechatronics.2022.102798.
[10] A.M. Rios, T. Niu, X. Carrera, D. Cole, B. Shyrokau, MPC-Based haptic shared steering driving, IEEE/ASME Trans. Mechatron. 26 (3) (2021) 1201–1211, https://doi.org/10.1109/TMECH.2021.3063902.
[11] X. Wang, X. Hua, F. Xiao, Y. Li, X. Hu, P. Sun, Multi-object detection in traffic scenes based on improved SSD, Electronics 7 (11) (2018) 302, https://doi.org/10.3390/electronics7110302.
[12] M. Razzok, A. Badri, I. El Mourabit, Y. Ruichek, A. Sahel, Pedestrian detection and tracking system based on deep-SORT, YOLOv5, and new data association metrics, Information 14 (4) (2023) 218, https://doi.org/10.3390/info14040218.
[13] V. Rajaram, S.C. Subramanian, Heavy vehicle collision avoidance control in heterogeneous traffic using varying time headway, Mechatronics 50 (2018) 328–340, https://doi.org/10.1016/j.mechatronics.2017.11.010.
[14] K. Zhao, J. Deng, D. Cheng, Real-time moving pedestrian detection using contour features, Multimed. Tools Appl. 77 (2018) 30891–30910, https://doi.org/10.1007/s11042-018-6173-4.
[15] Gavrila D.M. Pedestrian detection from a moving vehicle. Pedestrian detection from a moving vehicle. In Computer Vision—ECCV 2000: 6th European Conference on Computer Vision Dublin, Ireland, June 26–July 1, 2000 Proceedings, Part II 6 (pp. 37-49). Springer Berlin Heidelberg.
[16] M. Razzok, A. Badri, I. El Mourabit, Y. Ruichek, A. Sahel, A new pedestrian recognition system based on edge detection and different census transform features under weather conditions, IAES Int J. Artif. Intell. 11 (2) (2022) 582–592, https://doi.org/10.11591/ijai.v11.i2.pp582-592.
[17] M. Razzok, A. Badri, I. El Mourabit, Y. Ruichek, A. Sahel, Pedestrian detection under weather conditions using conditional generative adversarial network, IAES Int. J. Artif. Intell. 12 (4) (2023) 1557–1568, https://doi.org/10.11591/ijai.v12.i4.pp1557-1568.
[18] D. Tian, Y. Han, B. Wang, T. Guan, W. Wei, A review of intelligent driving pedestrian detection based on deep learning, Comput. Intell. Neurosci. 2021 (2021) 5410049, https://doi.org/10.1155/2021/5410049.
[19] Y. Xiao, K. Zhou, G. Cui, L. Jia, Z. Fang, X. Yang, Q. Xia, Deep learning for occluded and multi-scale pedestrian detection: A review, IET Image Proc. 2021 15 (2) (2021) 286–301, https://doi.org/10.1049/ipr2.12042.
[20] Y. Sumi, B.K. Kim, M. Kodama, Evaluation of detection performance for safety-related sensors in low-visibility environments, IEEE Sens J. 21 (17) (2021) 18855–18863, https://doi.org/10.1109/JSEN.2021.3089207.
[21] T. Kim, S. Kim, Pedestrian detection at night time in FIR domain: comprehensive study about temperature and brightness and new benchmark, Pattern Recognit. 79 (2018) 44–54, https://doi.org/10.1016/j.patcog.2018.01.029.
[22] P. Tumas, A. Nowosielski, A. Serackis, Pedestrian detection in severe weather conditions, IEEE Access 8 (2020) 62775–62784, https://doi.org/10.1109/ACCESS.2020.2982539.
[23] Z. Wang, J. Feng, Y. Zhang, Pedestrian detection in infrared image based on depth transfer learning, Multimed. Tools Appl. 81 (2022) 39655–39674, https://doi.org/10.1007/s11042-022-13058-w.
[24] F. Altay, S. Velipasalar, The use of thermal cameras for pedestrian detection, IEEE Sens. J. 22 (12) (2022) 11489–11498, https://doi.org/10.1109/JSEN.2022.3172386.
[25] P. Hurney, P. Waldron, F. Morgan, E. Jones, M. Glavin, Review of pedestrian detection techniques in automotive far-infrared video, IET Intell. Transp. Syst. 9 (2015) 824–832, https://doi.org/10.1049/iet-its.2014.0236.
[26] R.C. Miclea, C. Dughir, F. Alexa, F. Sandru, I. Silea, Laser and LIDAR in a system for visibility distance estimation in fog conditions, Sensors 20 (21) (2020) 6322, https://doi.org/10.3390/s20216322.
[27] Zhao F., Jiang H., Liu Z. Recent Development of Automotive LiDAR Technology, Industry and Trends. In Proceedings of the Eleventh International Conference on Digital Image Processing (ICDIP 2019), Guangzhou, China, 10–13 May 2019; Volume 11179, p. 111794A.
[28] Schalling F., Ljungberg S., Mohan N. Benchmarking lidar Sensors for Development and Evaluation of Automotive Perception. In Proceedings of the 2019 4th International Conference and Workshops on Recent Advances and Innovations in Engineering (ICRAIE), Kedah, Malaysia, 28–29 November 2019; pp. 1–6.
[29] S. Iftikhar, Z. Zhang, M. Asim, A. Muthanna, A. Koucheryavy, A.A. Abd El-Latif, Deep learning-based pedestrian detection in autonomous vehicles: substantial issues and challenges, Electronics 11 (2022) 3551, https://doi.org/10.3390/electronics11213551.
[30] C. Goodin, D. Carruth, M. Doude, C. Hudson, Predicting the influence of rain on LIDAR in ADAS, Electronics 8 (1) (2019) 89, https://doi.org/10.3390/electronics8010089.
[31] A. Carullo, M. Parvis, An ultrasonic sensor for distance measurement in automotive applications, IEEE Sens J. 1 (2001) 143, https://doi.org/10.1109/JSEN.2001.936931.
[32] T. Schlegl, T. Bretterklieber, M. Neumayer, H. Zangl, Combined capacitive and ultrasonic distance measurement for automotive applications, IEEE Sens J. 11 (2011) 2636–2642, https://doi.org/10.1109/JSEN.2011.2155056.
[33] J. Zhou, J. Shi, RFID localization algorithms and applications—a review, J. Intell. Manuf. 20 (2009) 695, https://doi.org/10.1007/s10845-008-0158-5.
[34] D. Fernandez-Llorca, R.Q. Minguez, I.P. Alonso, C.F. Lopez, I.G. Daza, M.A. Sotelo, C.A. Cordero, Assistive intelligent transportation systems: the need for user localization and anonymous disability identification, IEEE Intell. Transp. Syst. Mag. 9 (2017) 25–40, https://doi.org/10.1109/MITS.2017.2666579.
[35] I. Gresham, A. Jenkins, R. Egri, C. Eswarappa, N. Kinayman, N. Jain, R. Anderson, F. Kolak, R. Wohlert, S.P. Bawell, et al., Ultra-wideband radar sensors for short-range vehicular applications, IEEE Trans. Micro Theory Tech. 52 (2004) 2105–2122, https://doi.org/10.1109/TMTT.2004.834185.
[36] S. Kuutti, S. Fallah, K. Katsaros, M. Dianati, F. Mccullough, A. Mouzakitis, A survey of the state-of-the-art localization techniques and their potentials for autonomous vehicle applications, IEEE Internet Things J. 5 (2018) 829–846, https://doi.org/10.1109/JIOT.2018.2812300.
[37] I. Shopovska, L. Jovanov, W. Philips, Deep visible and thermal image fusion for enhanced pedestrian visibility, Sensors 19 (17) (2019) 3727, https://doi.org/10.3390/s19173727.
[38] Z.A. Shaikh, D. Van Hamme, P. Veelaert, W. Philips, Probabilistic fusion for pedestrian detection from thermal and colour images, Sensors 22 (2022) 8637, https://doi.org/10.3390/s22228637.
[39] P. Wei, L. Cagle, T. Reza, J. Ball, J. Gafford, LiDAR and camera detection fusion in a real-time industrial multi-sensor collision avoidance system, Electronics 7 (6) (2019) 84, https://doi.org/10.3390/electronics7060084.
[40] J. Alfred-Daniel, C. Chandru-Vignesh, B.A. Muthu, et al., Fully convolutional neural networks for LIDAR–camera fusion for pedestrian detection in autonomous vehicle, Multimed. Tools Appl. 2023 (2023), https://doi.org/10.1007/s11042-023-14417-x.
[41] E.A. King, A. Tatoglu, D. Iglesias, A. Matriss, Audio-visual based non-line-of-sight sound source localization: a feasibility study, Appl. Acoust. 171 (1)) (2021) 107674, https://doi.org/10.1016/j.apacoust.2020.107674.
[42] A. Izquierdo, L. Del Val, J.J. Villacorta, W. Zhen, S. Scherer, Z. Fang, Feasibility of discriminating UAV propellers noise from distress signals to locate people in enclosed environments using MEMS microphone arrays, Sensors 20 (3) (2020) 597, https://doi.org/10.3390/s20030597.
[43] A. Izquierdo, J.J. Villacorta, L. Del Val, L. Suárez, Design and evaluation of a scalable and reconfigurable multi-platform system for acoustic imaging, Sensors 16 (10) (2016) 1671, https://doi.org/10.3390/s16101671.
[44] L. Del Val, A. Izquierdo-Fuente, J.J. Villacorta, M. Raboso, Acoustic biometric system based on preprocessing techniques and linear support vector machines, Sensors 15 (6) (2015) 14241–14260, https://doi.org/10.3390/s150614241.
[45] A. Izquierdo, L. Del Val, J.J. Villacorta, Feasibility of using a MEMS microphone array for pedestrian detection in an autonomous emergency braking system, Sensors 21 (12) (2021) 4162, https://doi.org/10.3390/s21124162.

Alberto Izquierdo Received the B.Eng. degree (1990) and the Ph.D. degree (1993) in telecommunications engineering from the Polytechnic University of Madrid, Spain. He is Professor at the Signal Theory and Communications and Telematics Engineering Department of the University of Valladolid, Spain. He is the Chair of the Array Processing Group and he is member of the Institute of Advanced Production Technologies (ITAP) of the same University. His research interests include array processing, acoustic radar design and applications, vibrations, ADAS, fault detection, digital signal processing.

Lara del Val Received the B.Eng. degree (2003) and the Ph.D. degree (2008) in telecommunications engineering, and the M.Eng. degree in acoustic and vibrations engineering (2010) from the University of Valladolid, Spain. She is working as an Associate Professor at the University of Valladolid, currently at the Signal Theory and Communications and Telematics Engineering Department, and, from 2013 to 2022, at the Mechanical Engineering Department. She is a member of the Array Processing Group and of the Institute of Advanced Production Technologies (ITAP) of the same University. Her research interests include array processing, acoustics, ADAS, fault detection and machine learning.

Juan J. Villacorta Received the B.Eng. degree (1996) and the Ph.D. (2002) in telecommunications engineering from the Valladolid University, Spain. He is currently working as an Associate Professor at the Signal Theory and Communications and Telematics Engineering Department of the University of Valladolid, Spain. He is a member of the Array Processing Group and of the Institute of Advanced Production Technologies (ITAP) of the same University. His research interests include digital signal processing, design and implementation of acquisition systems, array processing and acoustic radar design.